Energy Conversion and Management 101 (2015) 94–105

Contents lists available at ScienceDirect

Energy Conversion and Management

journal homepage: www.elsevier.com/locate/enconman

Two-stage robust UC including a novel scenario-based uncertainty model for wind power applications

Eduardo Álvarez-Miranda [a,*], Camilo Campos-Valdés [a], Claudia Rahmann [b]

[a] Industrial Engineering Department, Universidad de Talca, Curicó, Chile
[b] Electrical Engineering Department, U. de Chile, Chile

ARTICLE INFO

Article history:
Received 28 January 2015
Accepted 16 May 2015
Available online 2 June 2015

Keywords:
Unit commitment
Robust optimization
Wind forecast errors
Bootstrap inference process
Wind power

ABSTRACT

The complex processes involved in the determination of the availability of power from renewable energy sources, such as wind power, impose great challenges in the forecasting processes carried out by transmission system operators (TSOs). Nowadays, many of these TSOs use operation planning tools that take into account the uncertainty of the wind-power. However, most of these methods typically require strict assumptions about the probabilistic behavior of the forecast error, and usually ignore the dynamic nature of the forecasting process.

In this paper a methodological framework to obtain Robust Unit Commitment (UC) policies is presented; such methodology considers a novel scenario-based uncertainty model for wind power applications. The proposed method is composed by three main phases. The first two phases generate a sound wind-power forecast using a bootstrap predictive inference approach. The third phase corresponds to modeling and solving a one-day ahead Robust UC considering the output of the first phase.

The performance of proposed approach is evaluated using as case study a new wind farm to be incorporated into the Northern Interconnected System (NIS) of Chile. A projection of wind-based power installation, as well as different characteristic of the uncertain data, are considered in this study.

1. Introduction and motivation

The incorporation of renewable sources in electricity production has unquestionable benefits; low operating costs, near zero emissions and stability of their prices, to mention a few of them. Nonetheless, and particular in the case of wind power, the high levels of variability and uncertainty involved impose new challenges, especially in the operational planning carry out by transmission system operators (TSOs) [1,2].

Generation planning is usually performed by solving the well-known Unit Commitment (UC) Problem [3–6]. The UC is a fundamental problem that has been exhaustively studied from a practical and theoretical point of view. The UC optimizes the operational costs of the system during a specific period of time ensuring that the produced power will satisfy a given level of demand. Traditionally, the technical constraints considered in the optimization process are related to the operational limits of the generation units (such as minimum and maximum power capacity, up and down ramp rates, among others), transmission capacity of the system, and operational security constraints for the whole system.

A critical issue when using wind energy from a UC perspective is having reliable models for short-term forecasting of wind-power (see [2,7, and the references therein]). Nowadays, many power systems with high levels of wind-power generation use UC planning approaches that take into account the inherent uncertainty due to wind-power forecasting (see, e.g., [8,9]).

Typically, forecasting errors are incorporated into the decision process by means of stochastic modeling techniques (e.g., [10,11]), or by rather simple approaches such as fixed intervals (e.g., [12–14]). The premise of decision-makers is that forecasting error is unavoidable and it must be incorporated into the decision-making process, precisely in order to reduce its effect and find reliable and/or robust solutions.

The use of stochastic techniques usually yields the definition of a set of wind-power scenarios (see, e.g., [15,16]), whose probability of occurrence must be known a priori. This requires very strict, and possibly artificial assumptions about the stochastic behavior of the wind forecast error (see, e.g., [10,8]). On the one hand, an accurate representation of the possible outcomes requires to generate many scenarios, burdening the computational efficacy of such model; on the other hand, if a wrong scenario selection is done (which is likely to occur), the resulting solution lacks of practical value [17]. Moreover, in [18], it is studied how the typical forecasting error models fail in representing its true behavior.

* Corresponding author at: Industrial Engineering Department, Universidad de Talca, Merced 437, Curicó, Chile. Tel.: +56 075 201706.
E-mail address: ealvarez@utalca.cl (E. Álvarez-Miranda).

http://dx.doi.org/10.1016/j.enconman.2015.05.039
0196-8904/

The use of closed *deterministic* intervals for modeling wind-power uncertainty is becoming a common practice with the outburst of Robust Optimization [19,12,20,21]. *Deterministic* means that no probability distribution is needed to characterize how the wind-power distributes within the interval. So, instead of optimizing a stochastic function, one is interested in optimizing a worst-case measure. Although this model avoids the need of assumptions regarding the stochasticity of the wind-power, it has some drawbacks. In order to capture all the possible outcomes of wind-power, one needs to define sufficiently wide intervals; in addition, the worst-case emphasis of the robust models leads to focus only on the midpoint or lower limit of the intervals, ignoring information contained in the whole interval. This behavior, that yields over-conservative solutions, has been somehow tackled by introducing the so-called uncertainty budget (see, e.g., [19,21]).

1.1. Contribution and paper outline

The main contribution of this paper is the development of a methodological framework for obtaining one-day ahead robust UC policies in power systems with wind-power penetration. The proposed framework is comprised by specially revised methods of forecasting, uncertainty modeling and mathematical optimization. As it will be shown with a real case study, the combination of these methods yield UC policies that perform reasonably well regardless the actual wind-power values.

The paper is organized as follows. In Section 2.1 the forecasting method proposed in this paper is presented; the obtained forecast data is then used in a scenario generation scheme which is presented in Section 2.2. In Section 2.3 a modeling approached based on the concept of budget of uncertainty is presented; in the same section, a Mixed Integer Linear Programming (MILP) model for the Two-Stage Robust UC problem (TSRUC) is formulated. The case study is described in Section 3. In Section 4 numerical results analyzing different aspects of the methodology are reported. Finally, conclusions and paths for future work are presented in Section 5.

2. Methodology

The methodological framework proposed in this paper is designed to generate one-day ahead Robust UC policies considering wind-power generation uncertainty. Such framework is composed by three elements: (i) a wind-power forecasting approach via bootstrapping, (ii) a technique for generating wind-power scenarios, and (iii) a two-stage robust optimization model. In Fig. 1 a block diagram of the proposed methodology is shown. As can be seen, the framework requires wind-power measurements as input, which will be first used for forecasting and then for defining the scenarios. These two phases of the methodology are referred to as *Uncertainty Modeling* phase, since it yields a scenario-based model of uncertain wind-power values. The generated scenarios are then introduced in the optimization model (TSRUC), whose constraints are given by the operational characteristics of the power system (e.g., generator capacities, generator ramps, power demand, etc.). The final result is a one-day ahead robust UC especially suitable for high levels of uncertainty.

In the following, each of the elements of the proposed approach will be described.

2.1. Wind-power forecast via bootstrapping

The core of the forecasting method is the use of the bootstrapping re-sample procedure proposed in [22] (and later used in different areas (see, e.g., [23,24])).

Suppose that it is required to forecast the wind-speed that will be observed, hourly, tomorrow (denoted as day D^*). The strategy assumes the existence of wind-speed measurements of a period of time (e.g, a whole week), including the day (D^*-1) in which the forecasting is being carried out. Based on this real data, *several* possible data realizations of the first time-window of τ periods are forecast; for instance if $\tau = 3$ and an hourly basis is considered, the first periods would be 01:00 h, 02:00 h and 03:00 h. Then, for each of these periods an *average* forecast value is calculated, these estimated values are aggregated to the real data set, and the same forecasting procedure is applied for the following $\tau = 3$ periods (e.g., 04:00 h, 05:00 h and 06:00 h). This procedure is performed sequentially, until forecasts for all periods of day D^* have been calculated. In this case, it will be said that the model is *refreshed* each τ periods (e.g., 3 h).

The forecasting procedure for the first τ periods (hours) of day D^* is done as follows:

- **Step 1** Given a series of wind speed data (e.g., of two days), which is assumed to be available, a time series model is fitted to it [25].[1] A result of this is shown in Fig. 2(a) between periods 0–48.
- **Step 2** The residuals of the model are then calculated, i.e., the differences between the real values (measurements) and those obtained from the fitted model.
- **Step 3** A bootstrap series using a recursion function (which is characterized by the time series parameters and the calculated residuals) is generated, and the linear estimates of the forecasting function are then calculated.
- **Step 4** A bootstrap *future* or *forecast path* (or series of values) is obtained for the next τ periods using the estimators calculated in Step 3. An example of a 3 h path of forecast data is shown in Fig. 2(a).
- **Step 5** Repeat $\mathcal{P}$ times Steps 3 and 4. This is depicted in Fig. 2(b), where the paths obtained for $\mathcal{P} = 30$ are shown.

Once the paths for the first τ hours are obtained, the average value for each period using the $\mathcal{P}$ paths is calculated (see dark blue[2] line in Fig. 2(b)), these values are "concatenated" to the real data (refreshment), and Steps 1–5 are performed again in order to obtained the $\mathcal{P}$ paths for the following τ periods.

As result of applying this process consecutively for the 24 h of day D^*, it is possible to obtain for each period, say t, an interval given by the maximum forecast value ws_t^{max} (for a given path $p_{max} \in \{1,\ldots,\mathcal{P}\}$) and the minimum forecast value ws_t^{min} (for a given path $p_{min} \in \{1,\ldots,\mathcal{P}\}$). Intuitively, due to the refreshment strategy, the interval $[ws_t^{min}, ws_t^{max}]$ (at the beginning of the a time-window) is expected to be narrower than the interval $[ws_{(t+\tau)}^{min}, ws_{(t+\tau)}^{max}]$. This, because it is likely that the *quality* of the forecasting decreases, i.e., the magnitude of the residuals increases, between period t and period $t+\tau$. This is shown in Fig. 3(a), where a summary of the forecast values is shown for a complete day. It is clear how the induced interval (see gray lines) becomes wider along the periods between refreshment points.

2.2. Scenario generation

The forecasting strategy described before yields to intervals that are likely to *contain* the real wind-speed that will be realized. Once these intervals are calculated, the intervals can be transformed

[1] For the considered data (see Section 4) an ARIMA model was used since it provided the best goodness-of-fit, which was measured by the AIC, ACF and FACF tests (see [25, for fruther details]). Note that different data sets might be characterized by different time series models.

[2] For interpretation of color in Figs. 2 and 3, the reader is referred to the web version of this article.

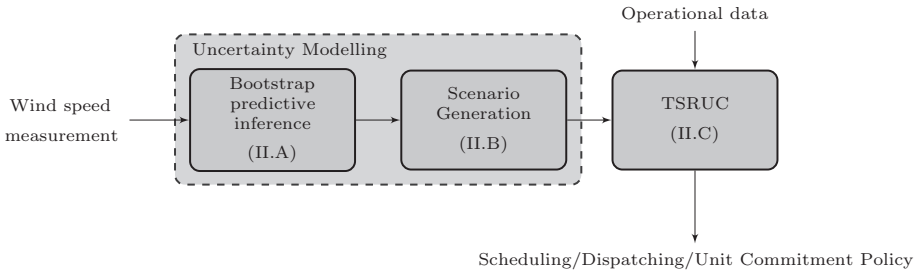

Fig. 1. Block model of the proposed methodology.

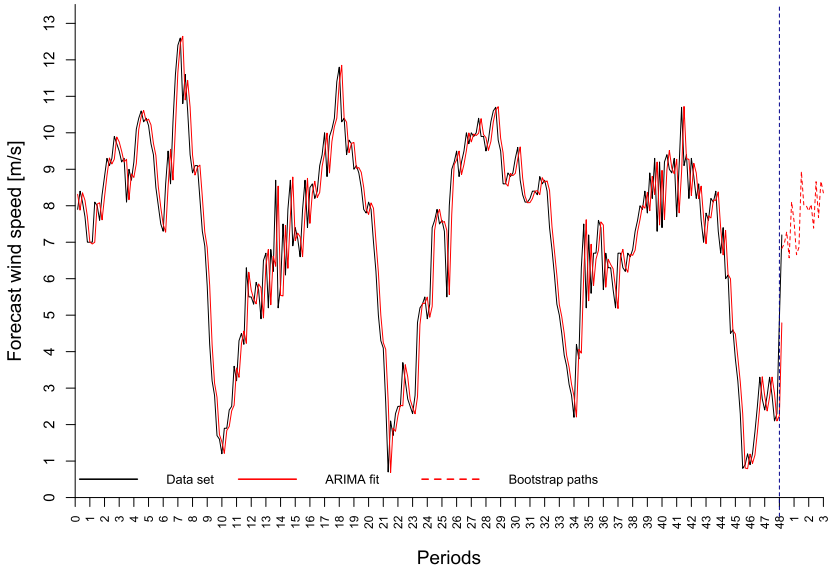

(a) Example of 1 bootstrapping-based forecast (01:00 - 03:00 hrs of November 21th, 2013)

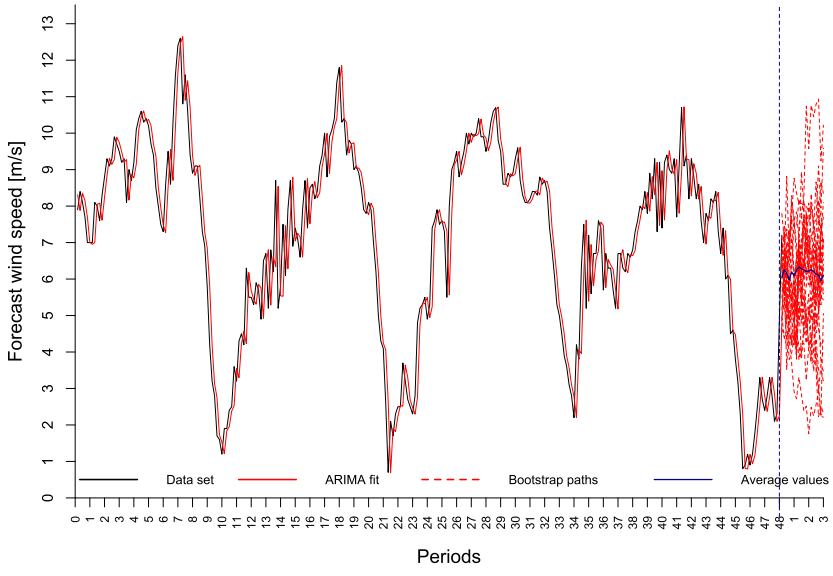

(b) Example of 30 bootstrapping-based forecasts (01:00 - 03:00 hrs of November 21th, 2013)

Fig. 2. Examples of the bootstrapping-based forecast procedure.

into wind power intervals $[q_t^{min}, q_t^{max}]$ (by choosing a wind power generator) and they can be incorporated into the decision model by means, for example, of an interval-data-based robust approach (see, e.g., [20,12]), or by means of a single-point scenario-based

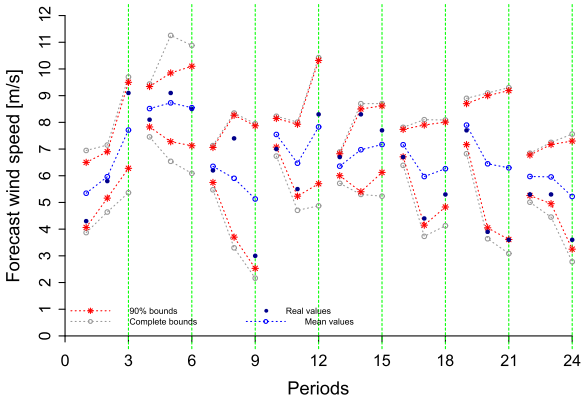

(a) Detailed representation of the forecasting for a complete 1-day period (November 21th, 2013)

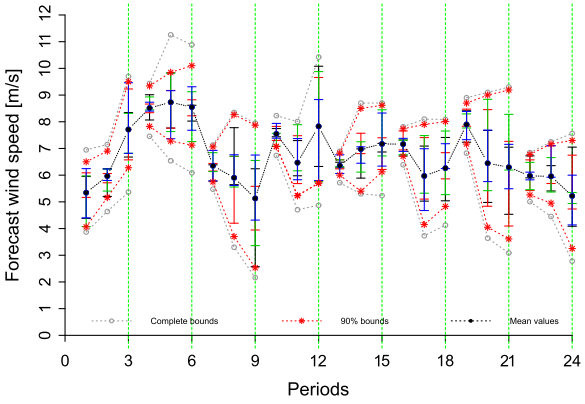

(b) Example of four interval-based scenarios (November 21th, 2013)

Fig. 3. Representation of the scenario generation.

(stochastic) method (see, e.g., [26,17]). The pros and cons of these alternatives are described in Section 1.

In this work, a scenario-based model of uncertainty that combines both uncertainty models mentioned above is proposed. In this novel model of uncertainty, a discrete set of scenarios is given, and each scenario is characterized by wind-speed *intervals*, one per period. In addition, no assumption is made with respect to the probability of occurrence of these scenarios nor the probability distribution of the values within the intervals. This model of uncertainty allows to cope two of the main drawbacks of the other two models: (i) intervals do not require to be *too* wide in order to capture the whole spectrum of values defined by the forecasting process, and (ii) only a reduced number of scenarios is enough to ensure that most of the possible realizations of values are sampled into the calculated scenarios.

The scenarios are generated as follows. After generating $\mathcal{P}$ bootstrapping *paths* (as described above), for each τ periods, a pair of paths that enclose at least the 90% of the forecast values is taken. Such pairs define an area that is likely to contain the true value of wind-speed in the corresponding period. This is depicted in Fig. 3(a), where these pairs are shown by red dashed lines and the true values are shown by dark blue points. Once these paths are calculated, a set of scenarios is defined; each of them characterized by one interval per period. These intervals have as midpoint the average value calculated considering the $\mathcal{P}$ bootstrapping estimations. The upper limits are randomly (and uniformly) taken between this average and the corresponding upper path; likewise, the lower limits are randomly (and uniformly) taken between this average and the corresponding lower path. In Fig. 3(b) an example of these interval-based scenarios is shown. In the figure four scenarios are depicted in green, blue, black and red, respectively. The dark blue points connected by dashed lines correspond to the aforementioned average values (and midpoint of the corresponding intervals). As one can see in this example (which corresponds to a day of the case study), only these four scenarios are enough to *cover* a broad spectrum of possible data realizations. This process is applied to generate a discrete set Ω of scenarios; for a given scenario $\omega \in \Omega$, $[q_t^{\omega-}, q_t^{\omega+}]$ corresponds to the uncertain interval (with midpoint $\bar{q}_t^{\omega}$) corresponding to the wind-power produced by a wind-power field of $\mathcal{U}$ generators at period t if scenario ω is realized. Note that no assumption is made regarding the probabilistic distribution of wind-power, nor about the probabilistic distribution of the forecasting error. This element is crucial when compared with other forecasting and error characterization techniques.

As it will be shown in Section 2.3, the two-stage robust optimization approach exploits this model of uncertainty by hedging against data realizations that are either *too* optimistic (i.e., high wind-speed) or *too* pessimistic (i.e., low wind-speed). Clearly, such cases might be induced by scenarios where wind-power is at the upper or lower interval limits, respectively. In this way, it is not only ensured that a *robust* fulfillment of the operating constraints and power demand, but the system is also protected against large fluctuations of wind-power output, which might induce problems in the system operation due to the violation of ramp constraints.

2.2.1. Comparison with persistence model

Currently, the TSO of the power system we will consider as a study case uses as forecasting model the well-known Persistence model (PM) (also called *naïve predictor*, see [18]). Intuitively speaking, the PM assumes that *tomorrow* (D^*) will happen what happened *today*. Although very simple, the PM is broadly used since it performs well for short prediction horizons (e.g., a few minutes or hours). Moreover, the PM is frequently used to compare the performance of newly proposed forecasting models. In Fig. 4 we show a schematic comparison between the PM and our scenario-based model. Real data of two days ($D^* - 1$ corresponds to November 19th, and D^* to November 20th) is shown with a black line; the PM used to forecast the wind speed of D^* is shown by a green line, and the overlapped intervals (and the corresponding midpoints) resulting of generating five scenarios are shown in blue. From this graphic it is possible to see that model proposed in this paper is able, in most cases, of *containing* the true values within the corresponding intervals. As it will be shown later, the fact that true values are contained within the intervals enable the optimization

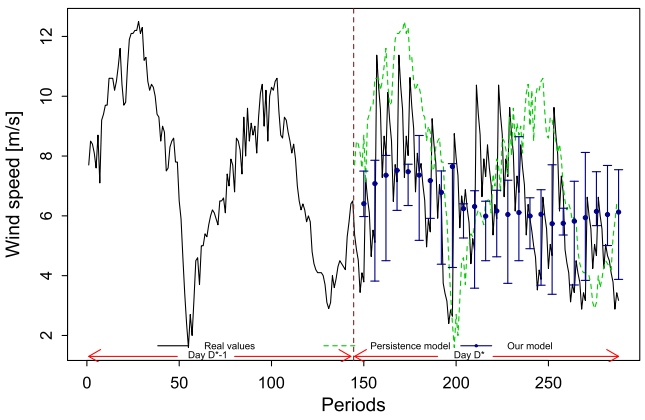

Fig. 4. Comparison between Persistence Model and our Scenario-based Model (November 20th).

model to provide, in average, more robust operation policies (in terms of their cost) than those provided by the PM.

2.3. An optimization model for the TSRUC

The third element of the methodology is modeling the Two-Stage Robust UC problem (TSRUC), using as input data the generated scenarios of the proposed uncertainty modeling phase.

2.3.1. Hedging against wind power fluctuation

So far, it has been presented a methodology to define a sound set of wind-speed scenarios that naturally embodies the uncertainty of wind-power. Now, it is necessary to develop a procedure to plug-in this information into the optimization framework. The method follows the idea of *budget of uncertainty* coined in [27], and it is a revisited version of the method applied for the same problem in [12].

Assume that day D^* is divided into T periods (for example, 24 periods of 1 h each). Now, for a given scenario $\omega \in \Omega$, there is an interval $[q_t^{\omega-}, q_t^{\omega+}]$ (with midpoint $\bar{q}_t^{\omega}$) for each period $t \in \{1,\ldots,T\}$. From the power generation point of view, a *good* data realization is such that the actual wind-power is $q_t^{\omega+}$; on the contrary, a *bad* one is $q_t^{\omega-}$.

Let Γ^+ be *maximum* number of periods that the wind-power is at the upper limit, and let Γ^- be *minimum* number of periods that the wind-power is at the lower limit. Therefore, if $\Gamma^+ = \Gamma^- = 0$, then it is assumed that all wind-power values will be at the corresponding midpoints; if $\Gamma^+ = 24$ and $\Gamma^- = 0$, then q_t can take any value within $[q_t^{\omega-}, q_t^{\omega+}]$; if $\Gamma^- = 24$ (and regardless the value of Γ^+), then wind-power values will be restricted to the corresponding lower bounds. Parameters Γ^+ and Γ^- enable the decision-maker to *control* the *level* of uncertainty so that the obtained solutions can be protected against scenarios with large fluctuations from the midpoints. Note that in [27], and later in [12], only one parameter Γ is considered, which in this context would correspond to Γ^+.

For better comprehension of the model, the following notation is needed: B, is the set of buses; Λ_b, is the set of generators at bus $b \in B$ ($\Lambda = \bigcup_{b\in B}\Lambda_b$); and Ω, is the set of scenarios $(\omega_1,\ldots,\omega_{|\Omega|})$.

Let $\mathbf{q} \in \mathbb{R}_{\geqslant 0}^{|B|\times|\Omega|\times T}$, be a vector of real-valued variables such that each element, q_{bt}^{ω}, indicates the actual wind-power used at bus b in period t, if the scenario ω is realized (MW). For simplicity, let $\hat{q}_{bt}^{\omega+} = (q_{bt}^{\omega+} - \bar{q}_{bt}^{\omega})$ and $\hat{q}_{bt}^{\omega-} = (\bar{q}_{bt}^{\omega} - q_{bt}^{\omega-})$. We define the auxiliary variables $\mathbf{z}^+ \in \{0,1\}^{|B|\times|\Omega|\times T}$ and $\mathbf{z}^- \in \{0,1\}^{|B|\times|\Omega|\times T}$, such that the wind-power output at given bus $b \in B$, at a given period $t \in \{1,\ldots,T\}$ and for a given scenario $\omega \in \Omega$, is at its upper limit ($z_{bt}^+ = 1$ and $z_{bt}^- = 0$), or at its lower limit ($z_{bt}^+ = 0$ and $z_{bt}^- = 1$), or at its midpoint ($z_{bt}^+ = z_{bt}^- = 0$). Variables $\mathbf{q}$, $\mathbf{z}^+$ and $\mathbf{z}^-$ are related as follows:

$$q_{bt}^{\omega} = \bar{q}_{bt}^{\omega} + \hat{q}_{bt}^{\omega+} z_{bt}^{+} - \hat{q}_{bt}^{\omega-} z_{bt}^{-}, \quad \forall t \in \{1,\ldots,T\},\ \forall b \in B \tag{Q.1}$$

$$\sum_{t=1}^{T} z_{bt}^{+} \leqslant \Gamma^{+} \text{ and } \sum_{t=1}^{T} z_{bt}^{-} \geqslant \Gamma^{-}, \quad \forall b \in B \tag{Q.2}$$

$$z_{bt}^{+} + z_{bt}^{-} \leqslant 1\ \forall t \in \{1,\ldots,T\}, \quad \forall b \in B \tag{Q.3}$$

$$(\mathbf{z}^{+}, \mathbf{z}^{-}) \in \{0,1\}^{2\times|B|\times|\Omega|\times T} \tag{Q.4}$$

Therefore, the corresponding uncertainty set, for a given scenario $\omega \in \Omega$, is given by

$$\mathcal{Q}^{\omega}(\Gamma^+,\Gamma^-) = \left\{\mathbf{q}^{\omega} \in \mathbb{R}_{\geqslant 0}^{|B|\times T} | (\text{Q.1})\text{–}(\text{Q.4})\right\} \tag{Q}$$

Intuitively, Γ^- controls the level of conservatism, and Γ^+ the level of optimism. This uncertainty set, which is determined by Γ^+ and Γ^-, will be then tackled when embedded into the mathematical optimization model presented next.

2.3.2. MILP Formulation for the TSRUC

In addition to the previously introduced notation, the following parameters will be used for the MILP formulation.

2.3.2.1. Parameters. T, number of time periods in the planning horizon, with each period $t \in \{1,\ldots,T\}$ being one hour; S_i^b, start-up cost for generator i at bus b (\$); SD_i^b, shut down cost for generator i at bus b (\$); G_i^b, (minimum-up time) minimum time that generator i, at bus b (h), must be operating after it is turned on; H_i^b, (minimum-down time) minimum time that generator i, at bus b (h), must be down after it is turned off; R_i^b, ramp-up limit for generator i at bus b (MW); P_i^b, ramp-down limit for thermal generator i at bus b (MW); L_i^b, minimal output of electricity if generator i at bus b is on (MW); U_i^b, maximal output of electricity if generator i at bus b is on (MW); D_t, total demand on the system in time period t (MW) (it also includes an estimation of the system losses); $q_{bt}^{\omega-}$, lower limit of the wind-power interval at bus b, in period t, if scenario ω is realized (MW); $q_{bt}^{\omega+}$, upper limit of the wind-power interval at bus b, in period t, if scenario ω is realized (MW); $\bar{q}_{bt}^{\omega}$, midpoint of the wind-power interval at bus b, in period t, if scenario ω is realized (MW).

The optimization problem is divided in two stages. The variable involved in each stage are follows.

2.3.2.2. Decision variables of first stage. $\mathbf{y} \in \{0,1\}^{|B|\times|\Lambda|\times(T+1)}$, vector of binary decision variables such that each element, y_{it}^b, indicates if generator i at bus b is on in period t ($y_{it}^b = 1$); $\mathbf{u} \in \{0,1\}^{|B|\times|\Lambda|\times T}$, vector of binary decision variables such that each element, u_{it}^b, indicates if generator i at bus b is started up in period t; $\mathbf{v} \in \{0,1\}^{|B|\times|\Lambda|\times T}$, vector of binary decision variables such that each element, v_{it}^b, indicates if thermal generator i at bus b is shut down in period t. Note that for practical purposes, $\mathbf{y}$ variables are also defined for $t = 0$.

2.3.2.3. Decision variables of second stage. $\mathbf{x} \in \mathbb{R}_{\geqslant 0}^{|B|\times|\Lambda|\times|\Omega|\times T}$, vector of real-valued variables such that each element, $x_{it}^{b\omega}$, indicates the amount of power generated by generator i at bus b in period t, if the scenario ω is realized (MW); $\boldsymbol{\delta} \in \mathbb{R}_{\geqslant 0}^{|B|\times|\Lambda|\times|\Omega|\times T}$, vector of real-valued variables such that each element, $\delta_{it}^{b\omega}$, indicates the amount of slack (unused) power of generator i at bus b in period t, if the scenario ω is realized (MW); $\mathbf{q} \in \mathbb{R}_{\geqslant 0}^{|B|\times|\Omega|\times T}$, vector of real-valued variables such that each element, $q_t^{b\omega}$, indicates the actual wind-power used at bus b in period t, if the scenario ω is realized (MW).

2.3.2.4. Generation cost function. The generation cost of a generator $i \in \Lambda_b$, at bus $b \in B$, in period $t \in \{1,\ldots,T\}$, and in scenario $\omega \in \Omega$, is given by the function $f_i^b : x_{it}^{b\omega} \to \mathbb{R}_{\geqslant 0}$, whose structure depends, in principle, on the type of generator. In this work a piecewise linear function has been considered.

As said before, the formulation defines a two-stage (robust) problem. In the first stage, the decision about the state of each generating unit (on/off) is defined. Intuitively speaking, it is decided *today* which generating unit will be working *tomorrow*, and for how long. In the second stage, the so-called *dispatching* problem has to be solved. This means that it is defined how much energy will be produced *tomorrow* by each of the committed generating units, taking into account the UC defined in the first stage, the power demand and the wind-power availability (the later subject

to the realized scenario). The goal is to find a cost efficient one-day ahead operation policy, i.e. a unit commitment schedule for tomorrow, such that it minimizes a worst-case measure of the operating cost of the second-stage decisions.

A first-stage UC must satisfy two operating constraints: (i) if a unit i at bus b is turned on, then it must remain on at least the minimum-up time (G_i^b); (ii) if a unit i at bus b is shut down, then it must remain down at least the minimum-down time (H_i^b). These two constraints are modeled as follows:

$$-y^b_{i(t-1)} + y^b_{it} - y^b_{ik} \leqslant 0, \qquad \forall b \in B, \forall i \in \Lambda_b, \forall t, k \in \left\{t, t+1, \ldots, G_i^b + t - 1\right\} \tag{FS.1}$$

$$y^b_{i(t-1)} - y^b_{it} + y^b_{ik} \leqslant 1, \qquad \forall b \in B, \forall i \in \Lambda_b, \forall t, k \in \left\{t, t+1, \ldots, H_i^b + t - 1\right\} \tag{FS.2}$$

$$-y^b_{i(t-1)} + y^b_{it} - u^b_{it} \leqslant 0, \qquad \forall b \in B, \forall i \in \Lambda_b, \forall t \in \{1, \ldots, T\} \tag{FS.3}$$

$$y^b_{i(t-1)} - y^b_{it} - v^b_{it} \leqslant 0, \qquad \forall b \in B, \forall i \in \Lambda_b, \forall t \in \{1, \ldots, T\} \tag{FS.4}$$

$$y^b_{i0} = 0, \qquad \forall i \in \Lambda_b, \forall b \in B \tag{FS.5}$$

$$\mathbf{y} \in \{0,1\}^{|B|\times|\Lambda|\times(T+1)}, \ \mathbf{u} \in \{0,1\}^{|B|\times|\Lambda|\times T} \quad \text{and} \quad \mathbf{v} \in \{0,1\}^{|B|\times|\Lambda|\times T} \tag{FS.6}$$

Constraints (FS.1) and (FS.2) model the two operating constraints described above. Constraints (FS.3) and (FS.4) relate variables y^b_{it}, u^b_{it} and v^b_{it}. Constraint (FS.5) defines the boundary conditions for any feasible units scheduling. Constraint (FS.6) imposes that all first-stage variables must be binary. Finally, note that the cost of the UC (in other words, the first-stage cost), is given by $g(\mathbf{y}, \mathbf{u}, \mathbf{v}) = \sum_{t=1}^{T} \sum_{b\in B} \sum_{i\in\Lambda_b} \left(S_i^b u^b_{it} + SD_i^b v^b_{it}\right)$.

Given a feasible UC, i.e., a collection $(\hat{\mathbf{y}}, \hat{\mathbf{u}}, \hat{\mathbf{v}})$ satisfying (FS.1)–(FS.6), a pair (Γ^+, Γ^-), and a scenario $\omega \in \Omega$, the corresponding second-stage dispatching problem is given by

$$\rho(\hat{\mathbf{y}}, \hat{\mathbf{u}}, \hat{\mathbf{v}}, \omega) = \min \sum_{t=1}^{T} \sum_{b=1}^{B} \sum_{i\in\Lambda_b} f_i^b(x^{b\omega}_{it}) \tag{DP.1}$$

$$\text{s.t. } L_i^b y^b_{it} \leqslant x^{b\omega}_{it} \leqslant U_i^b y^b_{it}, \quad \forall t \in \{1, \ldots, T\} \tag{DP.2}$$

$$x^{b\omega}_{it} - x^{b\omega}_{i(t-1)} \leqslant \left(2 - y^b_{i(t-1)} - y^b_{it}\right) L_i^b + \left(1 + y^b_{i(t-1)} - y^b_{it}\right) R_i^b, \quad \forall t \in \{2, \ldots, T\} \tag{DP.3}$$

$$x^{b\omega}_{i(t-1)} - x^{b\omega}_{it} \leqslant \left(2 - y^b_{i(t-1)} - y^b_{it}\right) L_i^b + \left(1 - y^b_{i(t-1)} + y^b_{it}\right) P_i^b, \quad \forall t \in \{2, \ldots, T\} \tag{DP.4}$$

$$x^{b\omega}_{it} \leqslant U_i^b - \delta^{b\omega}_{it} \text{ and } \delta^{b\omega}_{it} \leqslant U_i^b y^b_{it} \tag{DP.5}$$

$$\sum_{b=1}^{B} \sum_{i\in\Lambda_b} \delta^{b\omega}_{it} \geqslant \max_{i\in\Lambda_b, b\in B} \{x^{b\omega}_{it}\}, \quad \forall t \in \{1, \ldots, T\} \tag{DP.6}$$

$$\sum_{b=1}^{B} \left(\sum_{i\in\Lambda_d} x^{b\omega}_{it} + q^{b\omega}_t \right) \geqslant D_t, \quad \forall t \in \{1, \ldots, T\} \tag{DP.7}$$

$$\text{Constraints DP.2, DP.3, DP.4 hold} \quad \forall i \in \Lambda_b \text{ and } \forall b \in B \tag{DP.8}$$

$$\mathbf{q} \in \mathcal{Q}^{\omega}(\Gamma^+, \Gamma^-), \ \mathbf{x} \in \mathbb{R}^{|B|\times|\Lambda|\times|\Omega|\times T}_{\geqslant 0} \text{ and } \boldsymbol{\delta} \in \mathbb{R}^{|B|\times|\Lambda|\times|\Omega|\times T}_{\geqslant 0} \tag{DP.9}$$

The objective function (DP.1) corresponds to the minimum total generation cost of the units. In other words, it corresponds to the minimum dispatching cost induced by $\hat{\mathbf{y}}$, $\hat{\mathbf{u}}$, $\hat{\mathbf{v}}$ in case scenario ω is realized. Constraint (DP.2) ensures that if a generating unit is operative ($y^b_{it} = 1$), then it must produce at least L_i^b and at most U_i^b. Constraints (DP.3) and (DP.4) correspond to the ramp-up and ramp-down constraints, respectively.[3] Constraints (DP.5) and (DP.6) model the so-called $(N-1)$-primary-reserve constraints. This requirement ensures that, in every period, the system will be able to withstand the outage of the largest single generating unit without activating load shedding schemes [28]. This criterion is also used in several other works (see, e.g., [29,30]). Constraint (DP.7) imposes that the total generated power, including wind-power, is at least the total demand in every period plus system losses. Constraint (DP.8) ensures the correctness of the model, and constraint (DP.9) characterize the nature of the variables.

For a given first-stage solution $(\hat{\mathbf{y}}, \hat{\mathbf{u}}, \hat{\mathbf{v}})$ the *robust dispatching cost* $R(\hat{\mathbf{y}}, \hat{\mathbf{u}}, \hat{\mathbf{v}})$ corresponds to the maximum (minimum) dispatching cost among all $\omega \in \Omega$, i.e.,

$$R(\hat{\mathbf{y}}, \hat{\mathbf{u}}, \hat{\mathbf{v}}) = \max_{\omega\in\Omega} \rho(\hat{\mathbf{y}}, \hat{\mathbf{u}}, \hat{\mathbf{v}}, \omega) \tag{RD}$$

Combining (FS.1)–(FS.6), (DP.1)–(DP.9) and (RD), the Two-Stage Robust UC is formally defined as

$$OPT_{\mathcal{R}} = \sum_{t=1}^{T} \sum_{b\in B} \sum_{i\in\Lambda_b} \left(S_i^b u^b_{it} + SD_i^b v^b_{it}\right) + R(\hat{\mathbf{y}}, \hat{\mathbf{u}}, \hat{\mathbf{v}}) \tag{1}$$

$$\text{s.t.} \quad \text{(FS.1)}-\text{(FS.6) and (DP.1)}-\text{(DP.9)} \tag{2}$$

An optimal first-stage UC $(\mathbf{y}, \mathbf{u}, \mathbf{v})$ is robust because it guarantees that, regardless which scenario actually occurs, the second-stage dispatching decisions will be: (i) economically efficient (due to the minimization of the worst case); (ii) protected against large fluctuations of wind-power (which is given by the combined effect of (Γ^+, Γ^-)); and (iii) reliable with respect to possible errors of the wind-power forecasting (due to the tailored procedure to generate forecast data).

2.3.3. Algorithmic alternatives and further considerations

There is a plethora of algorithmic techniques for solving the UC and its corresponding Stochastic and Robust counterparts. Recent reformulation and exact approaches for obtaining optimal or near optimal solutions for different variants of the UC can be found in [31–34]. Likewise, specially tailored metaheuristics for the UC have been recently proposed in [35–40]. Due to the structure of both Stochastic and Robust UC, decomposition approaches such as Benders Decomposition are effective tools tackle to problem and provide good solutions. This type of approach can be found in [41,42,10] for the Stochastic UC, and in [12,20,13,14] for the Robust UC.

Besides wind power uncertainty, authors have addressed UC considering demand uncertainty (see, e.g. [43]), incorporating constraints on emissions with stochastic behavior (see, e.g. [44]), or combining transmission network decisions (see, e.g. [45]), to mention just few possible generalizations or extensions of the basic UC problem.

3. Power system under study: NIS

The electricity system in the northern part of Chile (NIS) is a small isolated 50 Hz system with a current peak load of 2200 MW. The system is characterized by a pure thermal generation mix with a total installed capacity of 4500 MW based on diesel, coal, natural gas and oil. The system load is characterized by 90% industrial load (mining industry), and the remaining 10% corresponds to residential customers.

[3] In this paper, ramp constraints combine ramp-rate limit restriction when a generator is on and first-hour/last-hour minimum generation restriction.

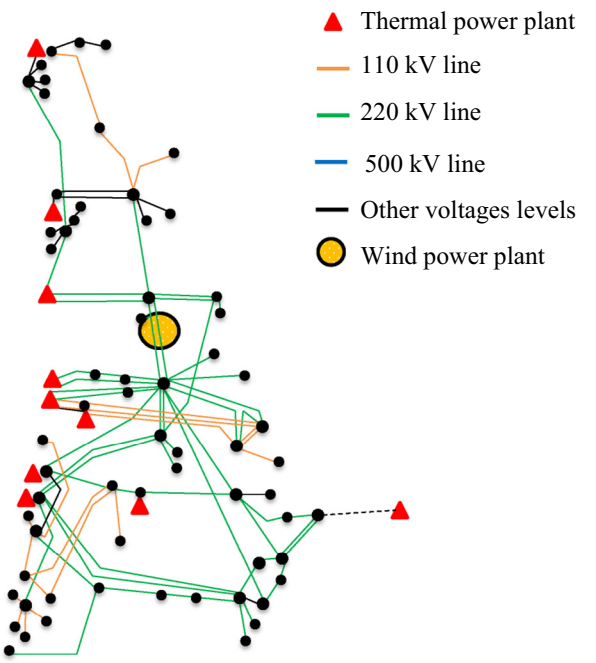

Fig. 5. Diagram of the NIS.

The case study considers 39 units based on diesel (41%), coal (33%), natural gas (21%) and oil (5%). Detailed technical information about the 39 units is provided in Table 2 in Appendix A. The purpose of this study is to evaluate a new wind-power plant connected to the NIS. This plant is expected to be located near the city of Sierra Gorda (latitude 22.92S, longitude 69.04E), an important area since many mines are located in the surroundings. Detailed wind-speed measurements from the studied area (for 2012 and 2013) are available in [46]. These measurements are incorporated into the forecasting machinery presented in Section 2.1 in order to generate wind-speed estimations for different days of 2013. The wind-power plant under evaluation is composed by Vestas V90-3.0 wind turbines (see [47]); settings of 33, 45 and 66 units (i.e., $\mathcal{U} = 33$, $\mathcal{U} = 45$ and $\mathcal{U} = 66$) will be considered as possible sizes of the wind-power plant. The wind-speed to wind-power conversion was made using the available datasheet of the turbine taking into account that the wind-speed measurements were made at 80 m and the turbine tower is 80 m tall. To illustrate the network structure and the location of the wind-power plant in the network, a simplified diagram of the NIS is shown in Fig. 5.

4. Numerical results

The experiments consist of solving the TSRUC, given by model (1) and (2), considering different input data: different days under study, different number of scenarios ($|\Omega|$), and different values of (Γ^+, Γ^-).

We have been provided with load data observed in 2013; since our goal is to assess the behavior of the model, the use of real demand records enables us to draw better conclusions. However, when finally implementing this method as part of the tools of the NIS management, load estimation will not represent an important challenge. This is justified due to the strong industrial characteristics of the NIS demand (load factor close to one), which leads to a quite flat load profile during the year [48].

Wind-power scenario sets for 12 different days (one day at random of every month) are generated. It has been considered $|\Omega| = 1$, $|\Omega| = 2$ and $|\Omega| = 5$ (1, 2 and 5 scenarios, respectively). Evidently, the larger the value of $|\Omega|$, the more possible data realizations are taken into account, and the better the quality of the corresponding optimal first-stage unit scheduling policy. Without loss of generality, it is assumed that for each of the selected days it is verified that $y^b_{i0} = 0$, for all $i \in \Lambda_b$ and for all $b \in B$.

The resulting MILP formulations are solved by means of the commercial solver CPLEX™ 12.5; this strategy proved to be successful for the data used in this work. Experiments were performed on an Intel Core™ i7 (4702QM) 2.2 GHz machine (8 cores) with 16 GB RAM. A time limit of 1200 s was imposed for every run of the code.

4.1. Sensitivity analysis

In order to analyze the performance of the model with respect to the different parameters, it has been performed a sensitivity analysis. The analysis consists of measuring the reduction of the operating costs derived by including the above discussed wind farm when compared to the operating cost of the current system (only fossil-fuel generators). The cost reduction is calculated with respect to the total cost (UC + dispatching/generation cost), the first-stage cost (the UC cost), and the second-stage cost (the dispatching/generation cost).

Total cost reductions induced by including wind power is an obvious effect. Therefore, the purpose of this sensitivity analysis is not to show that including renewables yields savings in the operation cost; instead, the goal is to show how the proposed robust optimization model is able to manage the uncertainty of wind power production according to the decision maker preferences regarding the level of uncertainty.

The experimental settings considers: (i) different values of $|\Omega|$ (1, 2 and 5); (ii) different values of (Γ^+, Γ^-) (0, 12 and 24, both of them).

In Table 1, the results obtained for $\mathcal{U} = 45$ and different combinations of $|\Omega|$ (column 1) and (Γ^+, Γ^-) (columns 2 and 3, respectively) are summarized. These results correspond to the average values calculated on the 12 studied days. Column "Red. total (%)" corresponds to the average reduction (expressed as a percentage) in the total operating cost (unit scheduling + dispatching), column "Red. 1stage (%)" corresponds to the reduction of the first-stage UC cost, and column "Red. 2stage (%)" shows the average reduction of the second-stage dispatching cost. Column "No. Cuts" reports the number of cutting planes added by CPLEX during the execution of the algorithm, column "No. Nodes" reports the number of branch-and-bound nodes explored by CPLEX, and column "Gap (%)" reports the optimality gap attained by CPLEX when reaching the time limit.

From Table 1, one can observe the following: (i) For a fixed value of $|\Omega|$ (number of scenarios) and a fixed value of Γ^+ (number of periods that wind-power can be at the upper limit), increasing the value of Γ^- (number of periods that wind-power can be at the lower limit) yields a diminishing of the total and second-stage cost reductions. (ii) For a fixed value of $|\Omega|$ and a fixed value of Γ^-, increasing the value of Γ^+ yields, generally, an augmentation of the total and second-stage cost reductions. (iii) For a fixed pair (Γ^+, Γ^-), increasing the value of $|\Omega|$ yields in a diminishing of the total and second-stage cost reductions. Intuitively speaking, these observations can be explained as follows: (i) if one assumes that more *bad* events can occur (by increasing Γ^-), then the max objective of the robust dispatching cost will *push-up* the dispatching costs (because Γ^- variables z^-_{bt} will be forced to be 1), resulting in a higher second-stage cost; (ii) if one assumes that more *good* events can occur (by increasing Γ^+), then the combined effect of the uncertainty set (more z^+_{bt} variables will

Table 1
Operating cost reductions and algorithmic performance, $\mathcal{U} = 45$.

$\|\Omega\|$	Γ^+	Γ^-	Red. total (%)	Red. 1stage (%)	Red. 2stage (%)	No. cuts	No. nodes	Gap (%)
1	0	0	3.10	3.00	3.11	664	101	0.30
1	0	12	2.85	3.76	2.81	718	321	0.17
1	0	24	1.72	1.06	1.75	675	93	0.34
1	12	0	4.33	3.26	4.37	703	367	0.19
1	12	12	3.82	4.03	3.81	692	290	0.21
1	12	24	1.72	1.06	1.75	679	104	0.33
1	24	0	4.75	3.22	4.81	657	90	0.34
1	24	12	3.81	3.67	3.82	710	451	0.16
1	24	24	1.72	1.06	1.75	680	105	0.32
2	0	0	3.07	2.47	3.09	1160	14	0.37
2	0	12	2.79	2.67	2.79	1215	18	0.38
2	0	24	1.66	1.07	1.68	1240	17	0.39
2	12	0	4.12	3.14	4.16	1193	19	0.37
2	12	12	3.64	3.03	3.66	1199	7	0.38
2	12	24	1.67	1.13	1.69	1240	17	0.38
2	24	0	4.50	3.75	4.53	1212	18	0.40
2	24	12	3.69	3.64	3.69	1202	19	0.32
2	24	24	1.66	1.04	1.68	1238	17	0.39
5	0	0	2.93	2.67	2.94	2712	2	0.54
5	0	12	2.49	1.79	2.52	2668	1	0.87
5	0	24	1.54	0.45	1.59	2772	3	0.51
5	12	0	3.47	1.15	3.57	2399	1	1.45
5	12	12	3.03	0.88	3.12	2189	1	1.80
5	12	24	1.53	0.19	1.59	2753	3	0.52
5	24	0	4.18	1.90	4.28	2795	3	0.58
5	24	12	3.10	1.24	3.18	2290	1	1.41
5	24	24	1.57	0.46	1.61	2755	3	0.49

tend to be 1) and the min objective of the TSRUC will *push-down* the dispatching cost; (iii) if more scenarios are considered, then a *new* worst-case scenario might appear, so a higher second-stage cost will be induced due to the definition of the *robust dispatching cost* (see (RD)).

From the values reported in the column "Red total (%)" it is possible to conclude that, if a wind farm of 45 units (135 MW) is incorporated into the current power system, the daily operative cost might experience an average reduction between 1.54 and 4.18%. Therefore, this type of analysis can be used by the TSOs for defining the values of Γ^- and Γ^+ that suit better to their preferences.

From column "Gap (%)", we can see that, in average, we have a guarantee that the obtained solutions are not further than 0.5% from the optimal ones. From columns "No. Cuts" and "No. Nodes", we see that the more scenarios we consider, the more difficult the problem becomes: more cutting planes have to be added to improve the bounds and less nodes are explored (because the linear programming relaxations become considerably harder).

From Table 1 it is possible to see that the proposed modeling and optimization strategy obtains sound results without any sophisticated implementation in quite reasonable running times (20 min), allowing real time applications. This means that the TSOs at NIS might not require complex algorithmic frameworks for obtaining their UC policies and, instead, they can use a more straightforward method as simply giving the resulting MILP formulation to a solver (such as CPLEX). As a matter of fact, one can retrieve detailed information of the units on/off scheduling by looking at the values attained by the $\mathbf{y}$ variables; likewise, the power that is expected to be produced by each unit can be also straightforwardly known by inspecting the $\mathbf{x}$ variables. In Table 3, in Appendix A, the generation hourly scheduling (corresponding to July 1st, 2013) of the 39 thermal units comprising the NIS is shown; likewise, the total power produced by these units, and its relation with respect to the total load and the wind power generation, is displayed in Fig. 9 in Appendix A.

4.1.1. Measuring robustness

When solving problem (1) and (2) with a particular setting of Ω, Γ^+ and Γ^-, one obtains *today* a scheduling of the working regime of (fossil-fuel) generators for *tomorrow*. Once the true wind-speed data is realized *tomorrow*, the obtained scheduling is expected to perform *well* in terms of the generation cost exhibited by the corresponding dispatching scheme.

To measure how well the obtained solutions actually perform, one needs more than just compare their cost with the cost induced by the system without the wind farm under evaluation. Indeed, one needs to test the obtained robust first-stage solution under many possible wind-speed realizations (and not only the worst-case scenario induced by the uncertainty sets $\mathcal{Q}^\omega$). This is done as follows:

Step 1 Calculate a first-stage UC $(\hat{\mathbf{y}}, \hat{\mathbf{u}}, \hat{\mathbf{v}})$, for a given day and a given uncertainty setting $(\Omega, \Gamma^+, \Gamma^-)$. Let $R(\hat{\mathbf{y}}, \hat{\mathbf{u}}, \hat{\mathbf{v}})$ be the *robust dispatching cost* (RD).

Step 2 Randomly generate a wind-power realization $\mathbf{s}$ contained in Ω.

Step 3 Calculate the optimal (second-stage) dispatching induced by $(\hat{\mathbf{y}}, \hat{\mathbf{u}}, \hat{\mathbf{v}})$ and the wind-power realization $\mathbf{s}$. Let $r(\hat{\mathbf{y}}, \hat{\mathbf{u}}, \hat{\mathbf{v}}, \mathbf{s})$ be the cost of the obtained dispatching.

Step 4 Calculate the relative difference between $R(\hat{\mathbf{y}}, \hat{\mathbf{u}}, \hat{\mathbf{v}})$ and $r(\hat{\mathbf{y}}, \hat{\mathbf{u}}, \hat{\mathbf{v}}, \mathbf{s})$ as

$$\Delta(\mathbf{s}) = \frac{R(\hat{\mathbf{y}}, \hat{\mathbf{u}}, \hat{\mathbf{v}}) - r(\hat{\mathbf{y}}, \hat{\mathbf{u}}, \hat{\mathbf{v}}, \mathbf{s})}{r(\hat{\mathbf{y}}, \hat{\mathbf{u}}, \hat{\mathbf{v}}, \mathbf{s})} \times 100\%.$$

Step 5 Repeat 250 times Steps 2–4. Let Δ the vector with all the values $\Delta(\mathbf{s})$ calculated in Step 4. (This number of replications has been decided for illustrative purposes.)

Clearly, if $\Delta(\mathbf{s}) > 0$ is obtained for a given realization $\mathbf{s}$, it means that the corresponding UC $(\hat{\mathbf{y}}, \hat{\mathbf{u}}, \hat{\mathbf{v}})$, along with the setting (Γ^+, Γ^-), *underestimates* the real wind-power potential because a cheaper dispatching can be obtained ($r(\hat{\mathbf{y}}, \hat{\mathbf{u}}, \hat{\mathbf{v}}, \mathbf{s}) < R(\hat{\mathbf{y}}, \hat{\mathbf{u}}, \hat{\mathbf{v}})$). On the contrary, if $\Delta(\mathbf{s}) < 0$, it means that the solution $(\hat{\mathbf{y}}, \hat{\mathbf{u}}, \hat{\mathbf{v}})$ and the setting (Γ^+, Γ^-), are such that *overestimate* the real wind-power potential (because the actual dispatching cost is more expensive). Therefore, a more robust setting (Γ^+, Γ^-) is the one that induces UC solutions verifying $\Delta(\mathbf{s}) \lessapprox 0$.

Some results obtained by carrying out the method described above are shown in Fig. 6. In this figure are displayed the boxplots of the values of associated with Δ, obtained for different combinations of (Γ^+, Γ^-) when having $|\Omega| = 1$ (Fig. 6(a)) and $|\Omega| = 5$ (Fig. 6(b)) (the graphics are obtained for July 1st). For each boxplot, both the maximum (above each boxplot) and average (marked with •) values are displayed. From the graphic, one can conclude the following: (i) for a fixed Γ^+, increasing Γ^- yields solutions that, in average, perform better (lower costs) than the corresponding worst-case (the differences tend to be greater than 0%); (ii) for a fixed Γ^-, increasing Γ^+ yields solutions that, in average, perform worse (highers costs) than the corresponding worst-case (the differences tend do be less than 0%), (iii) having 5 scenarios produces marginal differences in the results, meaning that a single scenario is already effective in capturing the nature of the uncertain data, at least for this particular data.

The above described behavior can be explained as follows: (i) Increasing Γ^-, forces the uncertainty set to be defined by more values at the lower bounds (yielding a higher dispatching cost); afterward, when generating a random scenario, this scenario is likely to be given by values that are greater than the lower limits, which induces a lower dispatching cost. (ii) Increasing Γ^+, allow the uncertainty set to be defined by more values at the upper limit

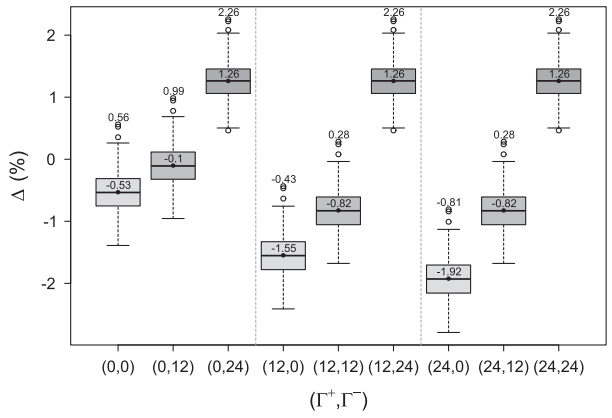

(a) $|\Omega| = 1, \mathcal{U} = 45$

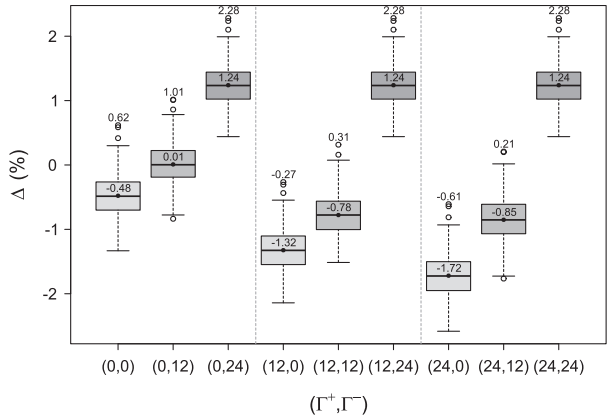

(b) $|\Omega| = 5, \mathcal{U} = 45$

Fig. 6. Boxplots of the differences between the worst-case dispatching cost and the optimal dispatching costs of 250 realizations (July 1st, 2013).

(yielding a lower dispatching cost); then, when generating a random realization, this realization is likely to be given by values that are less than the upper limits, which induces a higher dispatching cost.

The results shown in Fig. 6 allow to conclude that: (i) only if an over-conservative position is taken ($\Gamma^- = 24$) the obtained solutions systematically underestimate the actual potential of the wind-power generation ($\Delta > 0\%$); and, on the opposite side, (ii) models as those proposed in [12,21] ($\Gamma^- = 0$) will lead to (over-) optimistic solutions ($\Delta < 0\%$). The second behavior is explained by the effect of the max–min objective of the second-stage component (RD), which focuses only on those scenarios where the wind-power of Γ^+ periods is at the corresponding upper limit. The proposed model overcomes this two extreme cases by introducing two types of parameters to control the budget of uncertainty, Γ^+ and Γ^-, which leads to solutions that are better protected against different wind-power realizations, ensuring to be cost-efficient regardless the realized scenario. This is clear when looking at the boxplots obtained for $\Gamma^+ = 12$ and $\Gamma^- = 12$, where the values of Δ are closer to 0.0%.

4.2. Comparison with persistence model

In this part the proposed forecasting model is compared with the PM. In order to carry out the comparison, the following procedure is carried out.

Step 1 Calculate a first-stage UC $(\hat{\mathbf{y}}, \hat{\mathbf{u}}, \hat{\mathbf{v}})$, for a given day D^* and a given uncertainty setting $(\Omega, \Gamma^+, \Gamma^-)$. Let $R(\hat{\mathbf{y}}, \hat{\mathbf{u}}, \hat{\mathbf{v}})$ be the *robust dispatching cost* (RD).

Step 2 Calculate a first-stage UC $(\tilde{\mathbf{y}}, \tilde{\mathbf{u}}, \tilde{\mathbf{v}})$, for a given day D^* using the PM. Let $PM(\tilde{\mathbf{y}}, \tilde{\mathbf{u}}, \tilde{\mathbf{v}})$ be the corresponding dispatching cost.

Step 3 Calculate the optimal (second-stage) dispatching induced by $(\hat{\mathbf{y}}, \hat{\mathbf{u}}, \hat{\mathbf{v}})$ using the *real* wind-power values $\mathbf{r}$ of day D^* (which are assumed to be known). Let $r_1(\hat{\mathbf{y}}, \hat{\mathbf{u}}, \hat{\mathbf{v}}, \mathbf{r})$ be the cost of the obtained dispatching.

Step 4 Calculate the optimal (second-stage) dispatching induced by $(\tilde{\mathbf{y}}, \tilde{\mathbf{u}}, \tilde{\mathbf{v}})$ using the *real* wind-power values $\mathbf{r}$ of day D^*. Let $r_2(\tilde{\mathbf{y}}, \tilde{\mathbf{u}}, \tilde{\mathbf{v}}, \mathbf{r})$ be the cost of the obtained dispatching.

Step 5 Calculate $\Delta(r_1) = \frac{R(\hat{\mathbf{y}}, \hat{\mathbf{u}}, \hat{\mathbf{v}}) - r_1(\hat{\mathbf{y}}, \hat{\mathbf{u}}, \hat{\mathbf{v}}, \mathbf{s})}{r_1(\hat{\mathbf{y}}, \hat{\mathbf{u}}, \hat{\mathbf{v}}, \mathbf{r})} \times 100\%$, and $\Delta(r_2) = \frac{PM(\tilde{\mathbf{y}}, \tilde{\mathbf{u}}, \tilde{\mathbf{v}}) - r_2(\tilde{\mathbf{y}}, \tilde{\mathbf{u}}, \tilde{\mathbf{v}}, \mathbf{r})}{r_2(\tilde{\mathbf{y}}, \tilde{\mathbf{u}}, \tilde{\mathbf{v}}, \mathbf{s})} \times 100\%$.

Therefore, if a given setting $(\Omega, \Gamma^+, \Gamma^-)$ produces $\Delta(r_1) < \Delta(r_2)$, it means that the scenario-based uncertainty model allows to find a better solution than the one obtained with the PM.

In Fig. 7 are shown the results of applying Steps 1–5 for D^* = July 1st, considering different combinations of $(\Omega, \Gamma^+, \Gamma^-)$. From the results displayed in the Figure is clear that the proposed forecasting model leads to policies that respond better to wind-power variability than the solution obtained by the PM. An analysis of the results allows to draw the following conclusions: (i) only for over-conservative cases ($\Gamma^- = 24$) the obtained solution underestimates the real wind-power availability, $\Delta(r_1) > 0$; (ii) the PM fails in finding a good policy, yielding a solution that turns out to be more expensive than the one that would have been chosen if the true data would have been known in advance, $\Delta(r_2) > 0$.

4.3. The effect of including spinning reserves

To complement the results shown so far, the consideration of spinning reserves has been incorporated to the model. More precisely, constraint (DP.6) has been replaced by

$$\sum_{b \in B} \sum_{i \in \Lambda_b} \delta_{it}^{b\omega} \geqslant \max_{i \in \Lambda_b, b \in B} \{x_{it}^{b\omega}\} + O_t, \ \forall t \in \{1, \ldots, T\}, \qquad \text{(DP.6a)}$$

where O_t accounts for the spinning reserves. In particular, this term has been modeled as

$$O_t = \pi_1 D_t + \pi_2 \max_{\omega \in \Omega} \sum_{b \in B} q_t^{b\omega},$$

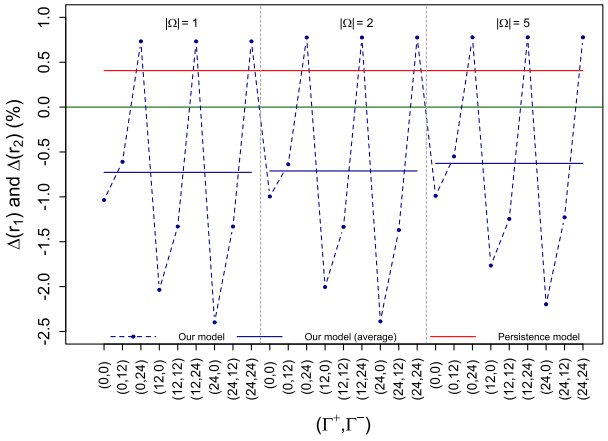

Fig. 7. Cost-based comparison between the PM and the proposed modeling framework ($\mathcal{U} = 45$, July 1st, 2013).

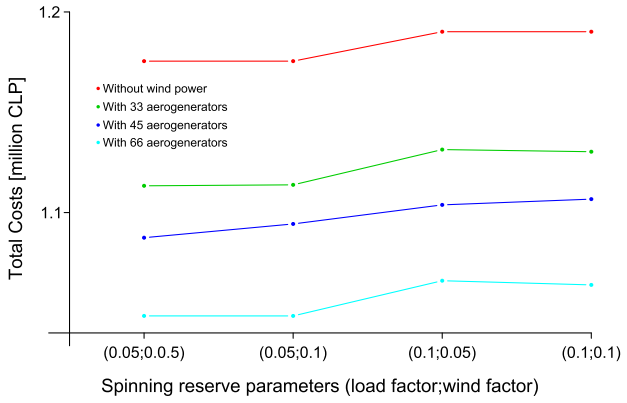

Fig. 8. Influence of different levels of Spinning Reserves on the total production cost considering different levels of wind power penetration (July 1st, 2013).

for $\pi_1 \in [0,1]$ (load factor) and $\pi_2 \in [0,1]$ (wind factor). This means that the spinning reserve at period t is equal to the π_1% of the total load at period t plus the π_2% of the total (maximum) wind-power expected at period t. By this way, we incorporate the fact that the additional amount of operating reserves required due to the variability and uncertainty of wind generation is dependent of its penetration level. This approach assumed a dynamic reserve requirement, i.e. one that is not constant for all hours of the optimization horizon but in fact a function of the wind penetration level. For these cases, it has been considered $\Gamma^- = 12$ and $\Gamma^+ = 12$.

The results obtained when considering $\pi_1,\ \pi_2 = \{0.5, 1.0\}$ (which leads to 4 combinations) are displayed in Fig. 8. Each curve, that corresponds to a given pair $\pi_1,\ \pi_2$, shows the relation between the total operating cost and different levels of wind power ($\mathcal{U} = 33,\ \mathcal{U} = 45$ and $\mathcal{U} = 66$).

The curves in Fig. 8 show that the way in which the spinning reserve O_t is defined has a direct impact on the total production cost of the system. However, since the considered wind penetration levels are not significant with respect to system demand D_t, increasing π_1 from 0.5 to 1.0 has a stronger influence on the total cost increase than increasing π_2 from 0.5 to 1.0.

This is an expected result from a power system perspective, since the difference between a wind farm of 33 or 66 wind turbines is not relevant when considering a total system demand of 2200 MW. Nevertheless for higher wind penetration levels the inclusion of the spinning reserves constraint should influence the total operating costs of the system.

Besides the impact on the total production cost, the incorporation of spinning reserves did not influence on the computational time.

5. Conclusions

In this paper a methodological framework to obtain Robust Unit Commitment policies, considering a novel scenario-based uncertainty model for wind power applications, is presented. The proposed method is composed by three main phases. The first two phases generate a sound wind-power forecast using a bootstrap predictive inference approach. The third phase corresponds to modeling and solving a one-day ahead Robust UC considering the output of the first phase.

The performance of the proposed framework was tested considering a new wind farm interconnected to the power system of the North of Chile. Using real data of wind-speed measurements, power demand and current generation infrastructure, robust UC policies were calculated for different parameter settings.

The obtained results suggest that the proposed methodology, as a whole, is effective in capturing the variability of wind-power and yielding unit commitment solutions that exhibit robustness. Moreover, the benefits of the proposed approach with respect to existing methods have been pointed out.

An important conclusion from the practical point of view, is that the methodological framework allows to obtain sound solutions, in short resolution times, and without any significant implementation effort, thus allowing it real time implementation.

As path for future work we would expect to apply this technique to other sources of renewable energies as photovoltaic or solar thermal power.

Acknowledgement

The authors acknowledge the support of the Chilean Council of Scientific and Technological Research, CONICYT, through the grants FONDAP N.15110019, FONDECYT N.11140060, and through the Complex Engineering Systems Institute (ICM: P-05-004-F, CONICYT: FBO16). The authors want to thank to A. Rodríguez (U. de Talca) for his invaluable comments and helpful discussions.

Appendix A

See Tables 2, 3 and Fig. 9.

Table 2
Detailed description of the 39 thermal units currently comprising the NIS.

Bus	Unit ID	Type	L_i^b (MW)	U_i^b (MW)	G_i^b (h)	H_i^b (h)	R_i^b (MW/h)	P_i^b (MW/h)
1	1	Diesel	95.00	120.35	1	1	10	10
	2	Diesel	95.00	120.35	1	1	10	10
	3	Diesel	120.00	135.30	1	2	8	8
	4	Diesel	95.00	122.76	1	1	10	10
	5	Diesel	95.00	117.75	1	1	10	10
	6	Diesel	82.90	135.30	1	2	8	8
	7	Diesel	2.10	14.32	1	1	40	1.6
	8	Diesel	0.65	2.68	1	1	0	0
	9	Diesel	0.85	6.62	12	1	10	0
	10	Diesel	10.00	42.11	5	1	10	0
	11	Diesel	2.00	27.92	5	1	3	0.1
	12	Diesel	8.00	98.98	1	1	0.22	1
	13	Diesel	1.03	10.86	1	1	10.32	1
2	14	Gas	115.00	204.95	6	1	13	13
	15	Gas	115.00	204.95	6	1	13	13
	16	Gas	115.00	222.81	24	4	7	7
	17	Coal	100.00	152.60	72	48	1	1
	18	Coal	150.00	244.03	48	48	2	5
	19	Coal	150.00	244.27	48	48	2.35	5
	20	Coal	100.00	153.90	72	48	1	1
3	21	Coal	90.00	154.90	120	48	3	3
	22	Coal	90.00	164.00	120	48	3	3
	23	Gas	100.00	151.56	1	1	6	6
	24	Gas	60.00	91.67	24	1	6	6
	25	Diesel	10.00	24.60	5	1	10	10
	26	Gas	75.00	275.10	1	1	14.5	14.5
	27	Gas	83.60	117.90	30	12	11.5	11.5
	28	Diesel	10.00	24.83	5	1	10	10
	29	Gas	10.00	37.20	5	1	10	10
	30	Fuel Oil No.6	15.00	36.00	24	8	6	6
	31	Fuel Oil No.6	15.00	36.00	24	8	6	6
4	32	Coal	50.00	79.58	48	24	4	4
	33	Coal	50.00	79.77	48	24	4	4
	34	Coal	75.00	127.67	48	24	5	5
	35	Coal	75.00	124.06	48	24	2	2
	36	Coal	65.00	127.44	48	48	3	3
	37	Coal	65.00	131.87	48	48	3	3
	38	Coal	100.00	148.52	48	48	0.75	3
	39	Diesel	8.00	23.65	1	1	10	10

Table 3
Hourly scheduling of the 39 thermal units comprising the NIS ($\Gamma^- = \Gamma^+ = 12$, $|\Omega| = 5$, $\mathcal{U} = 45$, July 1st, 2013).

	1	2	3	4	5	6	7	8	9	10	11	12	13	14	15	16	17	18	19	20	21	22	23	24
1	0	0	0	95	0	95	0	0	0	0	0	0	0	0	95	0	0	0	0	0	0	0	0	0
2	0	0	95	95	0	95	0	0	0	0	0	0	0	0	95	0	0	0	95	0	0	0	0	95
3	0	0	0	0	0	120	0	0	0	0	0	0	0	0	120	0	0	0	0	0	0	0	0	120
4	0	95	104	114	114	123	113	103	95	0	0	0	0	0	0	0	0	0	0	0	0	0	0	0
5	0	95	105	95	0	95	0	0	0	0	0	0	0	0	95	0	0	0	95	0	0	0	0	95
6	83	83	83	90	83	83	0	0	0	0	0	0	0	0	0	0	0	0	0	0	0	0	0	0
7	0	0	0	0	2	4	2	2	0	0	0	0	0	0	0	0	0	0	0	0	2	0	0	2
8	0	0	0	0	0	1	0	0	0	0	0	0	0	0	0	0	0	0	0	0	1	0	0	1
9	0	0	0	0	0	0	0	0	0	0	0	0	0	0	0	0	0	0	0	0	1	1	1	1
10	0	10	10	10	10	10	0	0	0	0	0	0	0	0	0	0	0	0	0	0	0	0	0	0
11	0	0	0	0	0	0	0	0	0	0	0	0	0	0	0	0	0	0	0	0	2	2	2	2
12	0	0	0	0	0	8	0	0	0	0	0	0	0	0	8	8	8	8	8	0	8	0	0	8
13	0	0	0	0	1	2	1	1	0	0	0	0	0	0	0	0	0	0	0	0	1	0	0	0
14	115	128	141	154	167	180	167	180	193	180	192	205	192	192	205	192	192	205	205	192	205	192	192	205
15	115	128	141	154	167	180	167	179	192	179	192	205	192	192	205	192	192	205	205	192	205	192	192	205
16	115	122	129	136	143	150	157	164	171	178	185	192	199	206	213	209	216	223	223	216	223	216	216	223
17	100	101	102	103	104	105	106	107	108	109	110	111	112	113	114	115	116	117	118	119	120	121	122	123
18	150	152	154	156	158	160	162	164	166	168	170	172	174	176	178	180	182	184	186	188	190	185	187	189
19	150	152	155	157	159	162	164	166	169	171	174	176	178	181	183	185	188	190	192	195	197	192	194	197
20	100	101	102	103	104	105	106	107	108	109	110	111	112	113	114	115	116	117	118	119	120	119	120	121
21	90	93	96	99	102	105	108	111	114	117	120	123	126	129	132	135	138	141	144	147	150	147	150	153
22	90	93	96	99	102	105	108	111	114	117	120	123	126	129	132	135	138	141	144	147	150	153	156	159
23	0	0	100	106	106	100	0	0	0	0	0	0	0	0	0	0	0	0	0	0	0	0	0	0
24	60	66	72	78	84	90	84	78	84	80	86	92	86	80	86	80	81	87	92	86	92	86	86	92
25	0	0	0	0	0	0	0	0	0	0	0	0	0	0	0	0	0	0	0	0	0	0	0	0
26	75	90	104	119	133	148	133	119	104	90	75	75	0	0	0	0	0	75	90	76	91	76	75	90
27	84	95	107	118	118	118	107	95	103	92	103	115	103	107	118	107	107	118	118	107	118	107	107	118
28	0	0	0	0	0	0	0	0	0	0	0	0	0	0	0	0	0	0	0	0	0	0	0	0
29	0	0	10	20	30	37	27	17	13	10	10	20	10	10	20	10	16	26	36	26	36	26	16	26
30	0	0	0	0	0	0	0	0	0	0	0	0	0	0	0	0	0	0	0	0	0	0	0	0
31	0	0	0	0	0	0	0	0	0	0	0	0	0	0	0	0	0	0	0	0	0	0	0	0
32	50	54	58	62	66	70	66	62	66	70	74	78	74	70	74	70	74	78	80	76	80	76	76	80
33	50	54	58	62	66	70	66	64	68	72	76	80	76	73	77	73	72	76	80	76	80	76	76	80
34	75	80	85	90	95	100	98	103	108	113	118	123	118	123	128	123	123	128	128	123	128	123	123	128
35	75	77	79	81	83	85	87	89	91	93	95	97	99	101	103	105	107	109	111	113	115	117	119	121
36	65	68	71	74	77	80	83	86	89	92	95	98	101	104	107	110	113	116	119	122	125	122	124	127
37	65	68	71	74	77	80	83	86	89	92	95	98	101	104	107	110	113	116	119	122	125	126	129	132
38	100	101	102	102	103	104	105	105	106	107	108	108	109	110	111	111	112	113	114	114	115	116	117	117
39	0	0	0	0	0	8	0	0	0	0	0	0	0	0	0	0	0	0	0	0	0	0	0	0

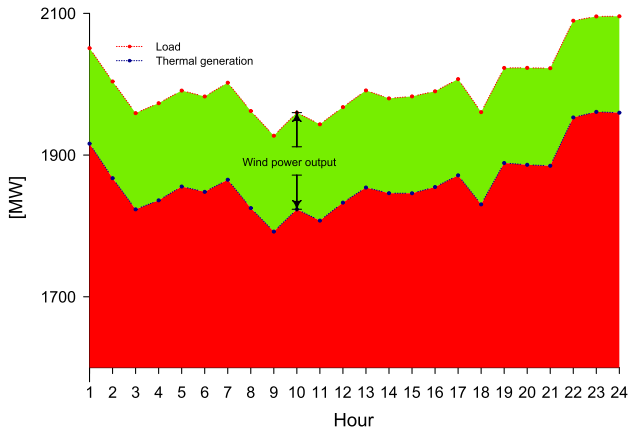

Fig. 9. Hourly-based comparison of total load (demand + losses + reserves, MW), the total thermal generation (MW), and the wind energy power (MW) ($\Gamma^- = \Gamma^+ = 12, |\Omega| = 5, \mathcal{U} = 45$, July 1st, 2013).

References

[1] Finardi E, Scuzziato M. Hydro unit commitment and loading problem for day-ahead operation planning problem. Int J Electr Power Energy Syst 2013;44(1):7–16.

[2] Giebel G, Brownsword R, Kariniotakis G, Denhard M, Draxl C. The state-of-the-art in short-term prediction of wind power: a literature overview. Technical report. ANEMOS.lus; 2011.

[3] Bertsekas D, Lauer G, Sandell N, Posbergh T. Optimal short-term scheduling of large-scale power systems. IEEE Trans Autom Control 1983;28(1):1–11.

[4] Baldick R. The generalized unit commitment problem. IEEE Trans Power Syst 1995;10(1):465–75.

[5] Sen S, Kothari D. Optimal thermal generating unit commitment: a review. Int J Electr Power Energy Syst 1998;20(7):443–51.

[6] Bisanovic S, Hajro M, Dlakic M. Unit commitment problem in deregulated environment. Int J Electr Power Energy Syst 2012;42(1):150–7.

[7] Wang X, Guo P, Huang X. A review of wind power forecasting models. Energy Proc 2011;12(0):770–8.

[8] Wang J, Botterud A, Bessa R, Keko H, Carvalho L, Issicaba D, et al. Wind power forecasting uncertainty and unit commitment. Appl Energy 2011;88(11):4014–23.

[9] Ela E, O'Malley M. Studying the variability and uncertainty impacts of variable generation at multiple timescales. IEEE Trans Power Syst 2012;27(3):1324–33.

[10] Huang Y, Zheng Q, Wang J. Two-stage stochastic unit commitment model including non-generation resources with conditional value-at-risk constraints. Electric Power Syst Res 2014;116(0):427–38.

[11] Kalantari A, Galiana F. Generalized sigma approach to unit commitment with uncertain wind power generation. Int J Electr Power Energy Syst 2015;65(3):367–74.

[12] Jiang R, Wang J, Guan G. Robust unit commitment with wind power and pumped storage hydro. IEEE Trans Power Syst 2012;27(2):800–10.

[13] Zhao C, Wang J, Watson J, Guan Y. Multi-stage robust unit commitment considering wind and demand response uncertainties. IEEE Trans Power Syst 2013;28(3):2708–17.

[14] Xiong P, Jirutitijaroen P. Two-stage adjustable robust optimisation for unit commitment under uncertainty. IET Gener Transm Distrib 2014;8(9):573–82.

[15] Xiang M, Zhou M, Zhang Z, Liu Y. Wind power multi-scenario state transition based unit commitment and reserve optimization. In: Proceedings of SUPERGEN 2012; 2012. p. 1–7.

[16] Nasrolahpour E, Ghasemi H. A stochastic security constrained unit commitment model for reconfigurable networks with high wind power penetration. Electric Power Syst Res 2014;121(0):341–50.

[17] Lowery C, O'Malley M. Impact of wind forecast error statistics upon unit commitment. IEEE Trans Sust Energy 2012;3(4):760–8.

[18] Hodge B, Milligan M. Wind power forecasting error distributions over multiple timescales. In: 2011 IEEE power and energy society general meeting; 2011. p. 1–8.
[19] Zhao L, Zeng B. Robust unit commitment problem with demand response and wind energy. In: 2012 IEEE power and energy society general meeting; 2012.
[20] Bertsimas D, Litvinov E, Sun X, Zhao J, Zheng T. Adaptive robust optimization for the security constrained unit commitment problem. IEEE Trans Power Syst 2013;28(1):52–63.
[21] Jiang R, Zhang M, Li G, Guan Y. Two-stage network constrained robust unit commitment problem. Euro J Oper Res 2014;234(3):751–62.
[22] Pascual L, Romo J, Ruiz E. Bootstrap predictive inference for arima processes. J Time Series Anal 2004;25(4):449–65.
[23] Pascual L, Romo J, Ruiz E. Bootstrap prediction intervals for power-transformed time series. Int J Forecast 2005;21(2):219–35.
[24] Kim J, Wong K, Athanasopoulos G, Liu S. Beyond point forecasting: evaluation of alternative prediction intervals for tourist arrivals. Int J Forecast 2011;27(3):887–901.
[25] Cryer J, Chan K. Time series analysis with applications in R. 2nd ed. Springer; 2008. Springer texts in statistics.
[26] Jiang H, Zhang S, Hu Z, Song Y, Chiwei Y. Robust optimization method for unit commitment with network losses considering wind uncertainties. In: 2012 IEEE power and energy society general meeting; 2012b.
[27] Bertsimas D, Sim M. Robust discrete optimization and network flows. Math Program 2003;Series B(98):49–71.
[28] Wood A, Wollenberg B, Sheble G. Power generation, operation, and control. 3rd ed. Wiley; 2013.
[29] Arroyo J, Galiana F. Energy and reserve pricing in security and network-constrained electricity markets. IEEE Trans Power Syst 2005;20(2):634–43.
[30] Hedman K, O'Neill R, Fisher E, Oren S. Optimal transmission switching with contingency analysis. IEEE Trans Power Syst 2009;24(3):1577–86.
[31] Rong A, Hakonen H, Lahdelma R. A dynamic regrouping based sequential dynamic programming algorithm for unit commitment of combined heat and power systems. Energy Convers Manage 2009;50(4):1108–15.
[32] Viana A, Pedroso J. A new milp-based approach for unit commitment in power production planning. Int J Electr Power Energy Syst 2013;44(1):997–1005.
[33] Amjady N, Ansari M. Hydrothermal unit commitment with AC constraints by a new solution method based on benders decomposition. Energy Convers Manage 2013;65:57–65.
[34] Tumuluru V, Huang Z, Tsang D. Unit commitment problem: a new formulation and solution method. Int J Electr Power Energy Syst 2014;57(0):222–31.
[35] Lee T, Chen C. Unit commitment with probabilistic reserve: an IPSO approach. Energy Convers Manage 2007;48(2):486–93.
[36] Yuan X, Su A, Nie H, Yuan Y, Wang L. Application of enhanced discrete differential evolution approach to unit commitment problem. Energy Convers Manage 2009;50(9):2449–56.
[37] Amjady N, Nasiri-Rad H. Security constrained unit commitment by a new adaptive hybrid stochastic search technique. Energy Convers Manage 2011;52(2):1097–106.
[38] Kuo C, Lee C, Sheim Y. Unit commitment with energy dispatch using a computationally efficient encoding structure. Energy Convers Manage 2011;52(3):1575–82.
[39] Ji B, Yuan X, Li X, Huang Y, Li W. Application of quantum-inspired binary gravitational search algorithm for thermal unit commitment with wind power integration. Energy Convers Manage 2014;87(0):589–98.
[40] Yuan X, Ji B, Yuan Y, Ikram R, Zhang X, Huang Y. An efficient chaos embedded hybrid approach for hydro-thermal unit commitment problem. Energy Convers Manage 2015;91(0):225–37.
[41] Carøe C, Ruszczynski A, Schultz R. Unit commitment under uncertainty via two-stage stochastic programming; 1997.
[42] Barth R, Brand H, Meibom P, Weber C. A stochastic unit-commitment model for the evaluation of the impacts of integration of large amounts of intermittent wind power. In: International conference on probabilistic methods applied to power systems; 2006. p. 1–8.
[43] Liu G, Tomsovic K. Robust unit commitment considering uncertain demand response. Electric Power Syst Res 2015;119(0):126–37.
[44] Laia R, Pousinho H, Melíco R, Mendes V. Self-scheduling and bidding strategies of thermal units with stochastic emission constraints. Energy Convers Manage 2015;89(1):975–84.
[45] Jalilzadeh S, Shayeghi H, Hadadian H. Integrating generation and transmission networks reliability for unit commitment solution. Energy Convers Manage 2009;50:777–85.
[46] Ministerio de Energía (Gobierno de Chile). Campaña de medición del recurso Eólico y Solar; 2014. <http://walker.dgf.uchile.cl/Mediciones/>.
[47] Vestas Wind Systems. V90-3.0 MW Turbine; 2014. <http://www.vestas.com/>.
[48] Centro de Despacho Económico de Carga del Sistema Interconectado del Norte Grande (CDEC-SING). Private Communication; 2014.